# Mechanism of Photocatalytic Production of Active Oxygens on Highly Crystalline $TiO_2$ Particles by Means of Chemiluminescent Probing and ESR Spectroscopy

**Tsutomu Hirakawa, Hiroshi Kominami,[†] Bunsho Ohtani,[‡] and Yoshio Nosaka***

*Department of Chemistry, Nagaoka University of Technology, Kamitomioka, Nagaoka 940-2188, Japan, Department of Applied Chemistry, Faculty of Science and Engineering, Kinki University, Higashi-Osaka, Osaka 577-0818, Japan, and Catalysis Research Center, Hokkaido University, Sapporo 060-0811, Japan*

*Received: April 9, 2001*

The effect of calcination on photocatalytic activities was studied for highly crystalline $TiO_2$ powder, which was synthesized by the method of hydrothermal crystallization in organic media (HyCOM). The productions of $O_2^{\bullet-}$and $H_2O_2$ under ambient condition were monitored by means of luminol chemiluminescence probing. The amount of produced $O_2^{\bullet-}$ was decreased with the calcination at lower temperatures in parallel to the decrease of inner $Ti^{3+}$ signal observed at 77 K by ESR spectroscopy. The formation route for $H_2O_2$ under aerated condition is mainly two-step $O_2$ reduction in the presence of oxidizable organic molecules such as luminol. Oxidization activity was significantly high when HyCOM-$TiO_2$ was calcined at higher temperatures, 973−1173 K, as monitored by the amount of oxidized luminol. The observation in ESR measurements and other evidences indicated that the luminol is oxidized via hydroxyl radicals rather than the direct oxidation by photoinduced surface trapped holes.

## Introduction

Recently, $TiO_2$ photocatalysts have been studied with much attention because they can decompose and mineralize pollutant and/or undesirable compounds in air and wastewater.[1−4] To propagate the practical application, development of highly active photocatalysts is indispensable. One of the strategies of making highly active $TiO_2$ is to give particles a high crystallinity and a large surface area. The former may reduce the possibility of electron ($e^-$)−hole ($h^+$) recombination at a defective site, while the latter enhance the adsorption of reaction substrates to react with $e^-$ and $h^+$. Kominami and co-workers have synthesized $TiO_2$ of high crystallinity and large surface area, as well as high thermal stability, by a newly developed method of hydrothermal crystallization in organic media (HyCOM).[5] The calcined HyCOM-$TiO_2$ has been reported to show high activities under deaerated conditions in various reactions, such as dehydrogenation of 2-propanol[6] and deposition of silver metal along with molecular oxygen evolution.[7] On the other hand, in aerated conditions and in the absence of a sacrificial reagent, mineralization of acetic acid is the only photocatalytic reaction reported with HyCOM-$TiO_2$.[8] Therefore, it is of interest to explore the photocatalytic activities of this highly crystallized $TiO_2$ for the other important reactions under aerated atmosphere.

In the photocatalysis with $TiO_2$ under aerated conditions, active oxygen species such as superoxide radical ($O_2^{\bullet-}$), hydroxyl radical ($OH^{\bullet}$), and hydrogen peroxide ($H_2O_2$) have been noticed as key species to initiate the reactions.[9] These species are produced photocatalytically as shown by the following equations.

$$TiO_2 + h\nu \rightarrow e^- + h^+ \quad (1)$$

$$e^- + O_2 \rightarrow O_2^{\bullet-} \quad (2)$$

$$h^+ + H_2O \rightarrow OH^{\bullet} + H^+ \quad (3)$$

$$O_2^{\bullet-} + H^+ + e^- \rightarrow HO_2^- \quad (4)$$

$$2O_2^{\bullet-} + H^+ \rightarrow HO_2^- + O_2 \quad (5)$$

$$OH^{\bullet} + OH^{\bullet} \rightarrow H_2O_2 \quad (6)$$

That is, $O_2^{\bullet-}$ and $OH^{\bullet}$ are produced by photocatalytic reduction of $O_2$ (2) and oxidation of $H_2O$ (3), respectively, and then $H_2O_2$ is produced by the reduction (4) or disproportionation (5) of $O_2^{\bullet-}$, as well as the dimerization of $OH^{\bullet}$ (6). In the (4) and (5), $HO_2^-$ is changed into $H_2O_2$ at usual pH since p$K_a$ of $H_2O_2$ is 11.7.

We have studied the relationship between the properties of $TiO_2$ powder and the photocatalytic productions of $O_2^{\bullet-}$ and $H_2O_2$ by means of the luminol chemiluminescent (CL) probe method.[10,11] The amounts of $O_2^{\bullet-}$ and $H_2O_2$ produced by $TiO_2$ photocatalysis were found to correlate well with the secondary particle size and the amount of OH groups in $TiO_2$ powder.[11] Since luminol molecules are also oxidized by the photocatalytic reaction, the formation of active oxygens should be analyzed as the reaction in the presence of the sacrificial electron donor. In some experimental procedures, however, we could monitor them in the absence of the sacrificial reagent as well.[11]

In the present paper, by using the luminol CL method and ESR spectroscopy, the photocatalytic activity of highly crystallized HyCOM-$TiO_2$ will be discussed in correlation with the effects of the heat-treatment. In addition, the activity will be

* To whom correspondence should be addressed. E-mail: nosaka@nagaokaut.ac.jp.
[†] Department of Applied Chemistry.
[‡] Catalysis Research Center.

10.1021/jp0112929 CCC: $20.00 
Published on Web 06/26/2001

**TABLE 1: Properties of $TiO_2$ Photocatalysts**

| name | calcination temp/K | anatase component/% | primary particle size[a]/nm | BET surface area[b]/$m^2$ $g^{-1}$ | secondary particle size/$\mu$m | amount of OH groups/wt % |
|---|---|---|---|---|---|---|
| HyCOM-non | − | 100 | 17 | 140 | 9.7 | 2.9 |
| HyCOM-573 | 573 | 100 | 18 | 133 | 8.9 | 2.2 |
| HyCOM-823 | 823 | 100 | 23 | 78 | 10.7 | 1.4 |
| HyCOM-973 | 973 | 100 | 39 | 34 | 5.1 | 0.7 |
| HyCOM-1073 | 1073 | 73 | 44 | 8 | 7.7 | 0.3 |
| HyCOM-1173 | 1173 | 13 | 56 | 3 | 5.5 | 0.1 |
| ST-01 | − | 100 | 7 | 320 | 3.7 | 5.2 |
| P25 | − | 80 | 32 | 49 | 1.1 | 1.8 |

[a] Calculated from line broading of the anatase (110) peak in XRD pattern. [b] Reference 8.

compared with those of commercially available photocatalytic $TiO_2$ samples, P25 (Degussa), and ST-01 (Ishihara).

## Experimental Section

**Materials and Characterization.** HyCOM-$TiO_2$ was synthesized by hydrothermal crystallization in organic media. The details of the synthesis method have been described previously.[5] The HyCOM-$TiO_2$ was calcined in an electric furnace at various temperatures under air atmosphere. The rising rate of temperature was as slow as 3 K $min^{-1}$. After being kept for 1 h at the desired calcination temperatures ranging from 573 to 1173 K, the powder was cooled to the room temperature in the electric furnace. We designate the calcined samples by attaching the calcination temperature such as HyCOM-573. On the other hand, the HyCOM-$TiO_2$ without calcination was named as HyCOM-non. Commercially available $TiO_2$ powders, Degussa P25 (Nippon Aerosil, Co. Ltd.) and ST-01 (Ishihara Techno, Co. Ltd.), were generous gifts from the corresponding manufacturers.

The primary particle size and the crystalline composition of the samples were measured by X-ray diffraction (XRD) with a MacScience M03XHF22. BET surface area was measured by a Micromesotechs flowsorbs (Shimadzu 2300) with $N_2$ gas as an adsorbate. The amount of OH groups of $TiO_2$ was calculated as the relative decrement of the weight from 423 to 873 K, which was recorded with a TG-DTA meter (Seiko SSC/5200). The secondary particle size of the samples was measured for the suspension in 0.01 M NaOH solutions as the mean Stokes diameter with a centrifugal size distribution meter (Shimadzu SA-CP3). The properties of $TiO_2$ obtained by the above measurements are listed in Table 1.

For ESR measurements, the $TiO_2$ sample was placed in an ESR sample tube of 5 mm diameter, and then the tube was degassed at $1 \times 10^{-3}$ Torr and sealed. The measurements were performed at 77 K with a JEOL ES−RE2X ESR spectrometer under photoirradiation with a 500 W mercury lamp (Ushio, USH 500D) through a band-pass filter (HOYA, U350).

**Method of Chemiluminescent Probing.** Fifteen milligrams of $TiO_2$ was suspended in a 1 cm × 1 cm Pyrex glass cell with 3.5 mL of 0.01 M NaOH aqueous solution of pH 11. The sample cell was mounted on a magnetic stirrer in a dark box. The light source for excitation of $TiO_2$ was a 150W Xe-lamp (Hamamatsu Photonics, C2499). The excitation wavelength was confined to 387 ± 11 nm or 360 ± 25 nm by using glass filters (HOYA), i.e., a pair of U330 and L39 for 387 nm or U360 for 360 nm. Incident light intensities measured with a photometer (Advantest, TQ8210) were 40 and 3 mW $cm^{-2}$, respectively. After the irradiation was switched off with a shutter, luminol CL intensity was monitored with a photon-counting photomultiplier tube (Hamamatsu, R2949). Details for the experimental setup have been described previously.[10]

The luminol CL method can be divided into two procedures; post-addition and pre-addition methods. In the post-addition method, 50 $\mu$L of 7 mM luminol solution was added with a syringe into the $TiO_2$ suspension immediately after the end of the irradiation. On the other hand, in the pre-addition method, the same amount of luminol solution was added in $TiO_2$ suspension before the irradiation.

Two schemes for the light irradiation were employed in the experiments. One is single irradiation and another is multiple irradiation. The single irradiation was adopted mainly for the post-addition method, in which the irradiation duration was varied. In the multiple irradiation, the irradiation duration was 10 s and the interval between irradiations was 50 s including 20 s for the CL measurement. This irradiation scheme was adopted mainly in the pre-addition method.

Luminol chemiluminescent reactions observed by these methods involve the following two reactions, (7) and (8), where $L^{\bullet-}$ and L are luminol radical and two-electron-oxidized luminol, respectively.

$$O_2^{\bullet-} + L^{\bullet-} + H^+ \rightarrow LO_2H^- \rightarrow AP^* \quad (7)$$

$$HO_2^- + L \rightarrow LO_2H^- \rightarrow AP^* \quad (8)$$

The reaction product, $LO_2H^-$, rapidly decomposes into the excited state of 2-aminophthalate (AP*) which emits the light at around 425 nm. Since the CL intensity is proportional to the formation rate of $LO_2H^-$, it is proportional to the concentration products $[O_2^{\bullet-}][L^{\bullet-}]$ and $[HO_2^-][L]$ for (7) and (8), respectively. Both reactions contribute to the total CL intensity as expressed by the following eq 9, where $k_7$ and $k_8$ are the rate constants of the corresponding reactions and $\Phi$ is the quantum yield for (8).[10]

$$d[AP^*]/dt = k_7[O_2^{\bullet-}][L^{\bullet-}] + \Phi k_8[HO_2^-][L] \quad (9)$$

The time profile of CL intensity was analyzed to consist of two decay-components corresponding to the two CL reactions. The fast-decay component, corresponding to the first term in eq 9, is dominant only in the post-addition method where the amount of $H_2O_2$ is so small that the second term is negligible. The intensity of the fast-decay component which decays exponentially at a rate of about 1 $s^{-1}$, is proportional to the amount of $O_2^{\bullet-}$ because the amount of $L^{\bullet-}$ is higher than that of $O_2^{\bullet-}$, although $L^{\bullet-}$ is mainly formed by auto-oxidation. Therefore, from the fast-decay component the amount of $O_2^{\bullet-}$ can be estimated. The slow-decay component with the decay rate of 0.1−0.3 $s^{-1}$ is dominant in the pre-addition method because a large amount of L is produced by photocatalytic oxidation of luminol. Since L reacts with $OH^-$ ions, at pH 11.0 L molecules decompose with the lifetime of 0.25 ms. Thus, the amount of L is represented as a quasi-stationary state. The details of the analysis procedure and kinetic simulation have been described in the previous paper.[10b]

**TABLE 2: Amounts[a] of $O_2^{\bullet-}$, and $H_2O_2$, and Oxidized Luminol (L) Produced for Various $TiO_2$ Photocatalysts, HyCOM, ST-01, and P25**

| | concentration of $O_2^{-\bullet}/10^{-13}$ M | | concentration of $H_2O_2/\mu M^b$ | | |
|---|---|---|---|---|---|
| sample name | excitation wavelength = 360 nm | excitation wavelength = 387 nm | luminol present | luminol absent | concentration of $L/10^{-19}$ M[b] |
| HyCOM-no | 5.32 | 0.39 | 23 | 13 | 0.24 |
| HyCOM-573 | 2.07 | 0.96 | 3 | 12 | 1.65 |
| HyCOM-823 | 2.17 | 0.78 | 16 | 8 | 0.26 |
| HyCOM-973 | 1.38 | 0.69 | 8 | 7 | 1.02 |
| HyCOM-1073 | 1.24 | 0.78 | 14 | 2 | 1.65 |
| HyCOM-1173 | 1.50 | 1.65 | 38 | 5 | 2.76 |
| ST-01 | 6.47 | 1.13 | 19 | 13 | 1.52 |
| P25 | 2.17 | 0.53 | 14 | 9 | 1.94 |

[a] Steady-state concentration for $O_2^{\bullet-}$ and L and the produced concentration in 10 s for $H_2O_2$. [b] Excitation wavelength was 387 nm.

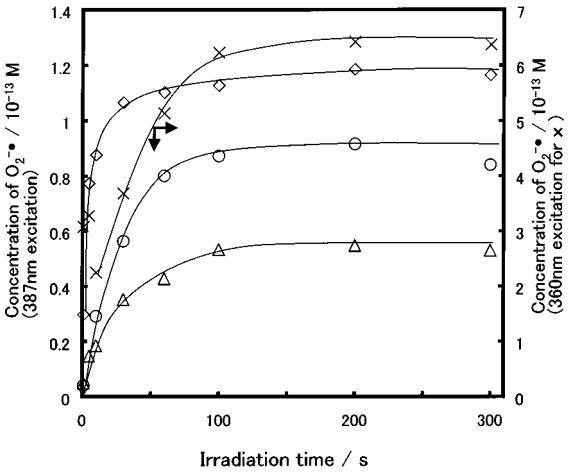


**Figure 1.** Concentration of $O_2^{\bullet-}$ estimated from chemiluminescence intensity of fast-decay component observed for several kinds of $TiO_2$ are shown as a function of irradiation time. Excitation wavelength is 387 nm for (◊) ST-01, (△) P25, and (○) HyCOM-823 are plotted on the left ordinate and at 360 nm for (×) ST-01 on the right ordinate.

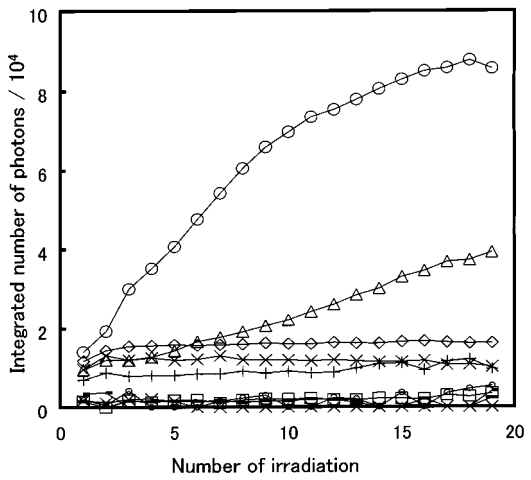


**Figure 2.** Chemiluminescence intensities for the two decay components observed in the pre-addition experiments. Observed number of photons are integrated over 20 s for each 10 s irradiation and plotted as a function of the number of irradiation. (○, HyCOM-1173; △, P25; ◊, HyCOM-973; ×, HyCOM-823; +, HyCOM-non) Slow-decay component (upper group) and fast-decay component (lower group) correspond to the relative amounts of $[H_2O_2][L]$ and $[O_2^{\bullet-}]$, respectively.

## Experimental Results

**Single Irradiation for the Luminol CL Method.** Figure 1 shows the amount of $O_2^{\bullet-}$ observed as a function of the duration time of the irradiation in the post-addition method for three kinds of $TiO_2$; ST-01, P25, and HyCOM-823. The amount of $O_2^{\bullet-}$ increased with irradiation and reached to a steady value at 100 s. Hereafter the irradiation duration of 100 s was employed in the single irradiation experiments. The amounts of $O_2^{\bullet-}$ observed for each $TiO_2$ by the irradiation at 360 and 387 nm are listed in Table 2. Although the light intensity of 360 nm is lower than that of 387 nm by a factor of 10 or more, the amount of $O_2^{\bullet-}$ with 360 nm excitation was smaller than that with 387 nm excitation. This difference can be explained by the different absorption coefficients at these wavelength.

**Multiple Irradiation for the Luminol CL Method.** Figure 2 shows the CL intensity observed after each irradiation on HyCOM-$TiO_2$ in the pre-addition method where luminol was added in advance. Only the 387 nm light was employed in the multiple irradiation experiment because the light of 360 nm can excite the luminol molecules as well as $TiO_2$.

The CL intensity of the fast-decay component is relatively small and shows no difference among the $TiO_2$ photocatalysts as shown in Figure 2. On the other hand, the CL intensity of the slow-decay component, which is governed by the amounts of L and $H_2O_2$, shows a significant difference. HyCOM-1173 causes a large increase in the CL intensity with the number of irradiation while P25 shows a moderate increase. On the other hands for HyCOM-non, -823, and -973 the CL intensity remains unchanged.

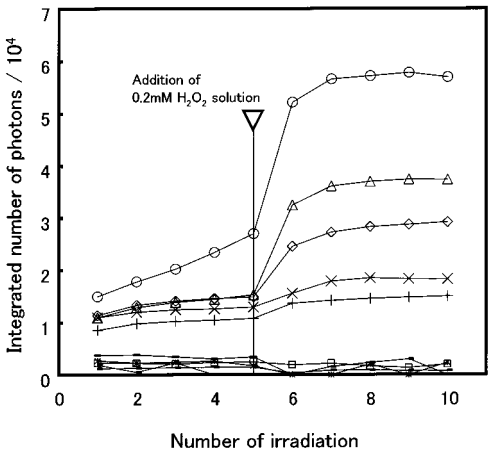


**Figure 3.** Addition of 0.2 mM $H_2O_2$ into the sample cell after the end of the 5-th irradiation in the pre-addition experiment of Figure 2. The experimental condition was same as Figure 2. (○, HyCOM-1173; △, P25; ◊, HyCOM-973; ×, HyCOM-823; +, HyCOM-non).

**Addition of $H_2O_2$ in the Multiple Irradiation.** Figure 3 shows the effect of the change in the $H_2O_2$ concentration. When 0.2 mM $H_2O_2$ was added in the above experiment, the CL intensity of the slow-decay component increased, while that of the fast-decay component remained almost unchanged. The increment of slow-decay component varied for different $TiO_2$, corresponding to the difference in the amount of produced L

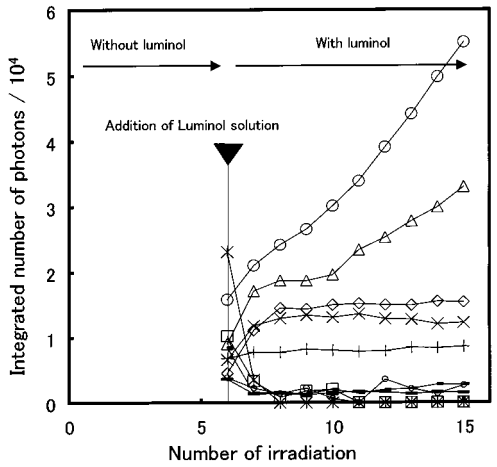


**Figure 4.** Chemiluminescence intensity of two decay components observed after repeated 10 s irradiations, where luminol was added immediately after the end of the sixth irradiation. (○, HyCOM-1173; △, P25; ◇, HyCOM-973; ×, HyCOM-823; +, HyCOM-non) Slow-decay component (upper group) and fast-decay component (lower group) correspond to the relative amounts of $[H_2O_2][L]$ and $[O_2^{\bullet-}]$, respectively.

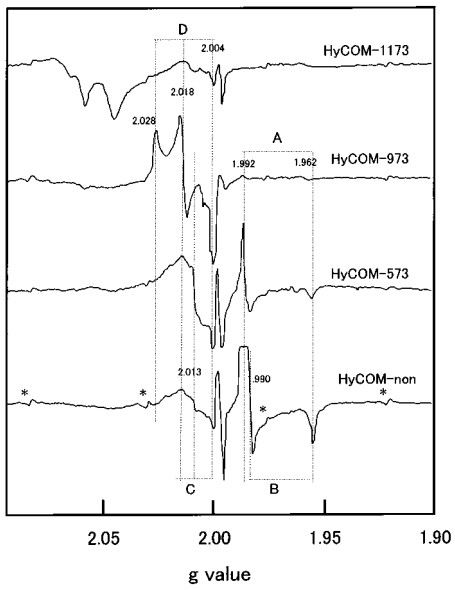


**Figure 5.** ESR spectra measured at 77 K under irradiation in a vacuum for HyCOM-$TiO_2$ powders calcined at several temperatures. (*: $Mn^{2+}$ marker).

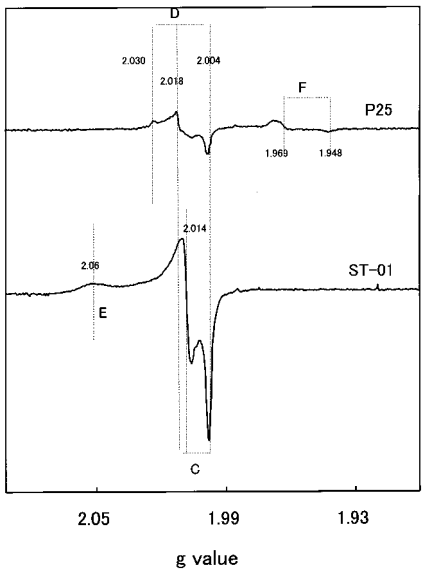


**Figure 6.** ESR spectra measured at 77 K under irradiation in a vacuum for P25 and ST-01 $TiO_2$ powders.

because the amount of added $H_2O_2$ was larger than that of $H_2O_2$ produced by $TiO_2$ photocatalysis. In addition, the amount of produced L is likely constant for each irradiation, as has been proved experimentally in the previous work for P25 $TiO_2$.[11] Thus, the amount of produced L can be calculated for each $TiO_2$ with the second term of eq 9 and then listed in Table 2. In this calculation, the CL intensity measured in the initial 20 ms was converted into the value of d[AP*]/d$t$ with the experimentally determined factor ($1.6 \times 10^{-18}$ M $s^{-1}$ for 1 photon/(20 ms)). The following parameters were adopted: $\Phi = 0.012$, $k_8 = 5 \times 10^7$ $M^{-1}$ $s^{-1}$, and $[HO_2^-] = 0.03$ mM.[10]

The amount of $H_2O_2$ produced by each 10 s irradiation could be calculated by comparing the increment in Figure 3 with the slopes in Figure 2. The concentration of $H_2O_2$ is listed in Table 2 as the value in the presence of luminol. For HyCOM-$TiO_2$, the production of $H_2O_2$ was increased with the calcination temperature and became higher than that for P25 and ST-01. In this experiment, the intrinsic ability of $H_2O_2$ formation for each $TiO_2$ could not be evaluated since luminol is oxidized simultaneously. Then the following experiment was performed.

**Addition of Luminol in the Multiple Irradiation.** Figure 4 shows the CL intensity of two decay components observed in the multiple irradiation procedure where luminol was added immediately after the sixth irradiation. At the sixth irradiation, the CL intensity of the fast-decay component is large. Since the procedure at the sixth irradiation is the same as that for the single irradiation post-addition method described above, the fast-decay component was significant relative to the slow-decay component. After the seventh irradiation and later, the feature is similar to that in Figure 2. The CL intensity of the slow-decay component observed at the seventh irradiation in Figure 4 is larger than that observed at the first irradiation in Figure 2, indicating that $H_2O_2$ is produced during six 10-s irradiations in the absence of luminol. Thus, from this difference in the CL intensity, the amount of $H_2O_2$ produced in the absence of luminol was calculated for one 10-s irradiation and listed in Table 2. This value was smaller than that in the presence of luminol for each $TiO_2$ and it decreases with increasing the calcination temperature.

**ESR Measurements.** Figures 5 and 6 represent the ESR spectra measured at 77 K under vacuum for HyCOM-$TiO_2$ calcined at various temperatures and for commercially available $TiO_2$, respectively. In Table 3, the assignment of the signals and the relative intensities were listed. The $g$ values obtained for calcined HyCOM-$TiO_2$ are in good agreement with those reported by Nakaoka and Nosaka for UV100 $TiO_2$, where signals B and F were not observed.[14] Signal B was assigned to inner $Ti^{3+}$ since the intensity was not changed with $O_2$ at 77 K. On the other hand, signal F with $g_1 = 1.948$, $g_2 = g_3 = 1.969$ was assigned to surface $Ti^{3+}$, which corresponds to the signal with $g_1 = 1.957$, $g_2 = g_3 = 1.990$ for UV100 $TiO_2$, since it was decreased in the presence of $O_2$ and increased with 2-propanol at 77 K. The signal B of HyCOM-$TiO_2$ was changed into signal A by the calcination, and this signal decreased gradually with increasing the calcination temperature and almost disappeared for HyCOM-$TiO_2$ calcined at 973 K. In the previous study, the signal A has been also assigned to inner $Ti^{3+}$ radical,[14] and signals C and D have been assigned to the subsurface hole and the surface hole,[14] respectively. The signal D appeared

**TABLE 3: The *g* Values of the ESR Signals Measured at 77 K, Their Assignment,[14] and the Relative Intensities for Each $TiO_2$ Sample**

| | | | | | signal intensity[a] | | | | | | | |
|---|---|---|---|---|---|---|---|---|---|---|---|---|
| | | g | | | HyCOM | | | | | | | |
| signal | assignment | $g_1$ | $g_2$ | $g_3$ | non | 573 | 823 | 973 | 1073 | 1173 | ST-01 | P25 |
| A | inner $Ti^{3+}$ | 1.962 | 1.992 | 1.992 | | 40 | 38 | 6 | | | | |
| B | inner $Ti^{3+}$ | 1.962 | 1.990 | 1.990 | 125 | | | | | | | |
| C | $Ti^{4+}-O^{\bullet-}-Ti^{4+}-OH^-$ | 2.004 | 2.014 | 2.018 | 6 | 12 | | | | | 20 | |
| D | $Ti^{4+}-O^{2-}-Ti^{4+}-O^{\bullet-}$ | 2.004 | 2.018 | 2.028 | | | 42 | 18 | 1 | | | 4 |
| E | $O_2^{\bullet-}$ | | | 2.06 | | | | | | | 4 | |
| F | surface $Ti^{3+}$ | 1.948 | 1.969 | 1.969 | | | | | | | | 1 |

[a] The signal intensity is represented as relative value to that of $Mn^{2+}$ marker at each characteristic *g* value which is 1.992, 1.990, 2.018, 2.028, 2.06, and 1.969 for signal A, B, C, D, E, and F, respectively.

newly by calcination at 823 K with the decrease of signal C, which is similar observation to the case of UV100 $TiO_2$.[14]

The signals at $g = 2.000$ and $g = 2.048-2.068$ were observed for HyCOM-1173 even without UV irradiation. These signals were not observed for calcined UV100 $TiO_2$ in the previous study.[14] Since the intensity of these signals was not changed with the irradiation, it may be attributable to paramagnetic species which are free from the photoinduced radicals although the assignment has been left to the further study.

As shown in Table 2, $TiO_2$ powders with a large amount of inner $Ti^{3+}$ at 77 K produced a large amount of $O_2^{\bullet-}$ at ambient temperature, although the inner $Ti^{3+}$ may promote the recombination. The existence of the correlation suggests that the photoinduced $e^- - h^+$ pairs in $TiO_2$ are stabilized separately at the corresponding trap sites at 77 K and then the $e^-$ trapped as inner $Ti^{3+}$ could not move to the surface or reaction site at the low temperature. At ambient temperature the inner $Ti^{3+}$ can react with $O_2$ molecules to produce $O_2^{\bullet-}$. This explanation is supported by the study of photoluminescence for anatase single crystal, where the behavior of the carriers at trap sites in $TiO_2$ varies by changing temperature with thresholds at 30 and 150 K.[17]

## Discussion

**$O_2^{\bullet-}$ Formation.** In the previous study, we showed that a higher amount of $O_2^{\bullet-}$ is produced photocatalytically with $TiO_2$ powders of a larger secondary particle size.[11] In the present study, the amount of $O_2^{\bullet-}$ produced by 360 nm irradiation did not show a monotonic change with the calcination temperature. Since $TiO_2$ of the calcined HyCOM did not show significant change in the secondary particle size as shown in Table 1, the present observation does not contradict to the conclusion in our previous report. When the excitation wavelength was 387 nm, the amount of $O_2^{\bullet-}$ increased with increasing the calcination temperature. This increase of $O_2^{\bullet-}$ for HyCOM of higher calcination temperatures above 973 K can be explained by the increase in the number of photons absorbed, since the absorption coefficient of anatase at 387 nm is small than that of rutile crystal. Moreover, although Table 1 shows almost same the physical properties for HyCOM-non and HyCOM-573, a high amount of $O_2^{\bullet-}$ was produced for HyCOM-non relative to HyCOM-573. Therefore, the calcination affects some other properties than those listed in Table 1.

It is probable that HyCOM-non contains an oxidizable organic compound since the titanium butoxide was used in the synthesis by HyCOM method.[5] To confirm the existence of organic compounds, thermal analysis for HyCOM-$TiO_2$ was carried out by the thermogravimetry (TG)−differential thermal analysis (DTA) apparatus. Figure 7 represents TG−DTA curves for as-prepared HyCOM-$TiO_2$. The sharp decrease in the TG curve

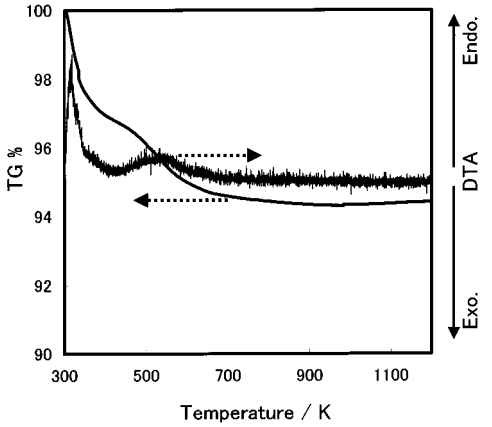


**Figure 7.** Thermogravimetry (TG) and DTA curve for as-prepared HyCOM $TiO_2$ (HyCOM-non) powder.

and an endothermic peak in the DTA curve at around 300 K to 430 K is attributable to the desorption of physisorbed water. At a higher temperature, a broad endothermic peak and a rapid weight loss were observed at the temperature around 530 K. This feature was also obtained for HyCOM-573 to a certain extent but not observed for HyCOM-$TiO_2$ calcined at the higher temperatures. These TG−DTA results suggest that butoxy groups are desorbed on the surface of the HyCOM-$TiO_2$ at 477−600 K. A similar result has been reported by Kambe et al.[15] They identified the exothermic peak at 493 K in their DSC measurement as *n*-butanol by GC−mass analysis and concluded that the *n*-butoxy groups exist on the surface of untreated HyCOM-$TiO_2$. In the present study, the number of *n*-butoxy groups on the surface of HyCOM-non was estimated from the weight loss in the TG curve. It was 1757 molecules per one $TiO_2$ particle of 17 nm diameter, or 5.8 molecules $nm^{-2}$ as the surface density. Thus, the existence of *n*-butoxy groups is responsible for the significant production of $O_2^{\bullet-}$ with HyCOM-non. That is, *n*-butoxy groups trap the photoinduced $h^+$ at the surface and then photoinduced $e^-$ becomes free from the recombination to increase the reduction of $O_2$.

The amount of $O_2^{\bullet-}$ produced by 360 nm excitation was decreased with the calcination at lower temperatures as summarized in Table 2, while the signal intensity of $Ti^{3+}$ also decreased as shown in Table 3. Then the intensity of inner $Ti^{3+}$ signal is plotted against the amount of $O_2^{\bullet-}$ as shown in Figure 8. The observation of linear correlation in Figure 8 indicates that $Ti^{3+}$ at 77 K is an electron trap site and capable to reduce $O_2$ to $O_2^{\bullet-}$ at room temperature. By calcination the carrier trap sites are removed and then the ESR signal becomes small.

ST-01 $TiO_2$ shows the highest activity in $O_2^{\bullet-}$ formation. The ESR spectrum for ST-01 in Figure 6 shows the formation of $O_2^{\bullet-}$ as signal E even at 77 K under vacuum condition, while

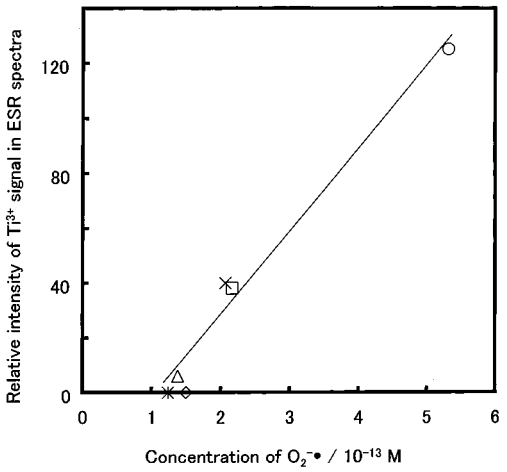


**Figure 8.** Relative amount of trapped electron $Ti^{3+}$ observed by ESR at 77 K is plotted as a function of the amount of $O_2^{\bullet-}$ produced in aqueous suspension at room temperature for various HyCOM-$TiO_2$ calcinated at various temperatures (○, no; ×, 573 K; □, 823 K; △, 973 K; ◇, 1073 K; □, 1173 K).

no signal of $Ti^{3+}$ radicals were observed. Therefore, the ST-01 $TiO_2$ can produce easily the $O_2^{\bullet-}$ even at 77 K because the primary particle size is so small for inner $Ti^{3+}$ to react with adsorbed $O_2$. On the other hand, the P25 $TiO_2$ shows the signal of surface $Ti^{3+}$ at 77 K and then produces $O_2^{\bullet-}$ at room temperature. The amount of $O_2^{\bullet-}$ is comparable to those of HyCOM-$TiO_2$ calcined at 573−823 K.

**Oxidation of Luminol.** As shown in Figure 3, the experimental result of $H_2O_2$ addition with the multiple irradiation allows us to estimate the amount of L produced by the photocatalytic reaction. The photocatalytic oxidation of luminol may take place as follows.

$$LH^- + h^+ \rightarrow L^{\bullet-} + H^+ \quad (10)$$

$$LH^- + OH^{\bullet} \rightarrow L^{\bullet-} + H_2O \quad (11)$$

$$L^{\bullet-} + h^+ \rightarrow L \quad (12)$$

$$2\,L^{\bullet-} + H^+ \rightarrow L + LH^- \quad (13)$$

$$L + OH^- \rightarrow \text{decomposition} \quad (14)$$

The potential of valence band holes is calculated to be 2.43 eV since the flat band potential of $TiO_2$ semiconductor at pH 11 is −0.77 V (NHE), based on the reported value of −0.12 V at pH 0.[12] Then irradiated $TiO_2$ is capable of easily oxidizing $LH^-$ because the redox potential for $L^{\bullet-}/LH^-$ is 0.798 V (NHE).[13] Hydroxyl radical OH which is formed photocatalytically from $H_2O$ (3) can also oxidize $LH^-$ (12) since $OH^{\bullet}/OH^-$ is 1.98 V (NHE). The resulting $L^{\bullet-}$ produces L, two-electron oxidized form of luminol, by further oxidation (11) or disproportionation (13). As stated above, since the produced L decomposes by $OH^-$ ion in ms, L is observed in a steady state.

The experimental result summarized in Table 2 shows that the amount of L was increased with increasing the calcination temperature. If the amount of L correlates with the BET surface area, the direct oxidation of $LH^-$ ion adsorbed on the $TiO_2$ surface can be expected. However, the surface area became small for the HyCOM-$TiO_2$ calcined at a higher temperature. The signal D in the ESR spectra, which is assigned to the surface trapped holes and having ability of direct oxidation, decreased gradually with increasing the calcination temperature. This observation is not consistent with the assumption that the surface trapped holes oxidized luminol directly. On the other hand, another trapped hole of signal C which has been assigned to the precursor of $OH^{\bullet}$ radical is observed for ST-01 and HyCOM-573. These $TiO_2$ produce relatively large amount of L. Since the surface of $TiO_2$ particles is negatively charged at pH 11, adsorption of $LH^-$ having the same charge would be difficult to occur. Then, the above experimental results suggest that luminol radical $L^{\bullet-}$ is not formed by the direct oxidation of $LH^-$ (10) but by the indirect oxidation with OH radicals (11).

**$H_2O_2$ Formation.** For almost all cases, the amounts of $H_2O_2$ produced in the presence of luminol became large as compared with in the absence of luminol. This experimental result shows that the recombination occurring between $e^- - h^+$ pairs or the primary products, $O_2^{\bullet-}$ and $OH^{\bullet}$, were suppressed by the increase of the photocatalytic oxidation of $LH^-$. In other words, the oxidation of $LH^-$ promotes the photocatalytic reduction of $O_2$. Then in the presence of luminol, $H_2O_2$ is formed mainly from $O_2^{\bullet-}$. Calcination at the lower temperatures caused a decrease in the amount of $H_2O_2$ produced with luminol, but it decreased at 1073−1173 K. The former decrease is attributable to the loss of surface butoxy groups and the latter increase is attributable to the increase of $O_2^{\bullet-}$ at 387 nm irradiation or the increase of oxidation ability represented by the increased amount of L produced. Without organic compounds such as luminol, the amount of $H_2O_2$ decreased gradually with the calcination temperature. This observation indicated that $H_2O_2$ is mainly produced from OH radicals which decreased by the reaction with $O_2^{\bullet-}$.

It seems possible that $H_2O_2$ is formed by dimerization of $OH^{\bullet}$ even in the presence of luminol since $OH^{\bullet}$ is present to oxidize luminol as stated above. To examine the effect of the dimerization of $OH^{\bullet}$, chloride ions, which scavenge photoinduced OH radicals, were used in the pre-addition method for P25 and ST-01 $TiO_2$. If the $H_2O_2$ is produced by dimerization of $OH^{\bullet}$, the amount of $H_2O_2$ should decrease on the addition of $Cl^-$ ions.[10] The experimental result showed that the CL intensity observed at each irradiation was not decreased with $Cl^-$ ions. Thus, it was confirmed that $H_2O_2$ was produced mainly from $O_2^{\bullet-}$ in the presence of sacrificial electron donors.

$O_2^{\bullet-}$ becomes $H_2O_2$, in two reaction pathways. One is the photocatalytic reduction (4) and another is the disproportionation of $O_2^{\bullet-}$ (5). This disproportionation is actually the reaction between $O_2^{\bullet-}$ and its protonated form, $HO_2^{\bullet}$ Since p$K_a$ of $HO_2^{\bullet}$ is 5.8, disproportionation at pH 11 seems difficult to occur. On the other hand, the photocatalytic reduction of $O_2^{\bullet-}$ may occur easily. Since the standard redox potential of the reaction 4 is +0.94 V (vs NHE),[16] $TiO_2$ photocatalyst has enough potential to the reduction of $O_2^{\bullet-}$ to $HO_2^-$ in aqueous solution even at pH 11. Thus, it is conclude that $H_2O_2$ is produced from $O_2$ in air by the two-step reduction.

In the absence of luminol, water is the only oxidizable species. Then $H_2O_2$ should be produced from $OH^{\bullet}$ radicals via eqs (3) and (6). The calcination at a higher temperature caused the increase in the oxidation ability represented by the increased amount of L produced, while the amount of $H_2O_2$ in the absence of luminol was not increased significantly. This observation is consistent with that $H_2O_2$ is mainly produced from OH radicals which decreased by the reaction with $O_2^{\bullet-}$. Note that for HyCOM-non the oxidation of butoxy group could be occur and $H_2O_2$ is produced from the two-step reduction of $O_2$.

On the basis of the amount of incident light, we can estimate the photonic efficiency to the production of $H_2O_2$. When two photons are absorbed in $TiO_2$, two $H_2O_2$ molecules are formally

produces in the absence of luminol and one $H_2O_2$ molecules are produced in the presence of luminol. By assuming that the light of 40 mW at 387 nm is completely absorbed in $TiO_2$ suspension of 3.5 mL without reflection, the absorbed photons in the unit of concentration are calculated to be 37 $\mu$M $s^{-1}$ or 370 $\mu$M for 10 s. Then the photonic efficiency of $H_2O_2$ formation for HyCOM-823 in the absence of luminol is calculated to be 2% (8 $\mu$M)and that for HyCOM-1173 in the presence of luminol to be 21% (38 $\mu$M). The actual photonic efficiency may be larger than these values because the reflection of anatase in water is about 11%, and the excitation wavelength is so broad that all the light may not be adsorbed.

## Conclusion

In the present work, the photocatalytic formations of $O_2^{\bullet-}$ and $H_2O_2$ were studied by the luminol CL probe method and ESR spectroscopy for highly crystallized $TiO_2$ powders produced by HyCOM method. The fact that the amount of $O_2^{\bullet-}$ produced by photocatalysis of HyCOM-$TiO_2$ was decreased with increasing the calcination temperature when excitation wavelength was 360 nm. This observation indicates the decrease of trap sites, which was evidenced by the ESR observations at 77 K where $Ti^{3+}$ signal was decreased with the calcination temperature. Although this ESR signal is assigned to inner $Ti^{3+}$ radical, it may not move to the surface or active site due to the stabilization at 77 K but reacts with $O_2$ adsorbed on the surface at room temperature. Without calcination HyCOM-$TiO_2$ has butoxy groups on the surface and produces a large amount of $O_2^{\bullet-}$ by 360 nm excitation, indicating that the butoxy groups react with the photoinduced $h^+$ to prevent the recombination of $e^- - h^+$ pairs.

The capability of $H_2O_2$ production on HyCOM-$TiO_2$ was different in the presence and the absence of luminol. In the presence of luminol, the production pathways for $H_2O_2$ are mainly the two-step reduction of $O_2$. On the other hand, in the absence of luminol, dimerization of $OH^{\bullet}$ may be dominant since the amount of $H_2O_2$ produced was decreased with the increase of $O_2^{\bullet-}$. The photonic efficiencies were more than 21% and 2% in the presence and the absence of luminol, respectively.

ESR observations supported the fact that luminol is oxidized preferably by $OH^{\bullet}$ radicals rather than the direct oxidation of surface $h^+$. $TiO_2$ synthesized by HyCOM method and calcined at 1173 K showed higher activity than commercially available photocatalytic $TiO_2$, ST-01 and P25, in the productions of $O_2^{\bullet-}$ and $H_2O_2$ and the oxidation of luminol by 387 nm irradiation. On the other hand, ST-01 and P25 $TiO_2$ showed a higher activity than HyCOM-$TiO_2$ in the $O_2^{\bullet-}$ formation by 360 nm irradiation and $H_2O_2$ formation in the presence of luminol.

**Acknowledgment.** The present work is partly defrayed by the Grant-in-Aid for Scientific Research on Priority-Area-Research from the Japanese Ministry of Science, Education and Culture.

## References and Notes

(1) (a) Fujishima, A.; Rao, T. N.; Tryk, D. A. *J. Photochem. Photobiol. C: Photochem. Rev.* **2000**, *1*, 1−21. (b) Fujishima, A.; Hashimoto, K.; Watanabe, T. *Photocatalysis*; BKC, Inc.: Tokyo, 1999. (c) Kaneko, M., Okura, I., Eds. *Photocatalysis-Science and Technology*; Kodansha-Scientific: Tokyo, 2001. In press

(2) . O'Shea, K. E.; Pernas, E.; Saiers. J. *Langmuir*, **1999**, *15*, 2071−2076.

(3) (a) Lindner, M.; Theurich, J.; Bahnemann, D. W. *Water Sci. Technol.* **1997**, *35*, 79−86. (b) Bekbolet, M.; Lindner, M.; Weichgrebe, D.; Bahnemann, D. W. *Sol. Energy* **1996**, *56*, 455−469.

(4) Mills, A.; Davies, R, H.; Worsley, D. *Chem. Soc. Rev.* **1993,** 417−425.

(5) (a) Kominami, H.; Takada, Y.; Yamagiwa, H.; Kera, Y.; Inoue, M.; Inui, T. *J. Mater. Sci. Lett*. **1996**, *15*, 197−200. (b) Kominami, H.; Murakami, S−y; Ohtani, B. Chapter 3 in ref 1c.

(6) Kominami, H.; Matsuura, T.; Iwai, K.; Ohtani, B.; Nishimoto, S.; Kera, Y. *Chem. Lett*. **1995**, 693−694.

(7) Kominami, H.; Murakami, S.; Kera, Y.; Ohtani, B. *Catal. Lett*. **1998**, *56*, 125−129.

(8) Kominami, H.; Kato, J.; Kohno, M.; Kera, Y.; Ohtani, B. *Chem. Lett*. **1996**, 1051−1052.

(9) (a) Hoffmann, M. R.; Martin, S. T.; Choi, W.; Bahnemann, D. W. *Chem. Rev.* **1995**, *95*, 69−96. (b) Serpone, N.; Pelizzetti, E.; Hidaka, H. In *Photocatalytic Purification and Treatment of Water and Air*; Ollis, D. F., Al-Ekabi, H., Eds.; Elsevier: London, 1993; pp 225−250.

(10) (a) Nosaka, Y.; Fukuyama *Chem. Lett.* **1997,** 383−384. (b) Nosaka, Y.; Yamashita, Y.; Fukuyama, H. *J. Phys. Chem. B* **1997**, *101*, 5822−5827. (c) Nosaka, Y. Chapter 5 in ref 1c.

(11) Hirakawa, T.; Nakaoka, Y.; Nishino, J.; Nosaka, Y. *J. Phys. Chem. B*, **1999**, *101*, 4399−4403.

(12) Duonghong, D.; Ramsden, J.; Graetzel, M. *J. Am. Chem. Soc*. **1982**, *104*, 2977−2985.

(13) Merenyi, G.; Lind, J.; Shen, X.; Eriksen, T. E. *J. Phys. Chem*. **1990**, *94*, 748−752.

(14) Nakaoka, Y.; Nosaka, Y. *J. Photochem. Photobiol. A.: Chem.* **1997**, *110*, 299−305.

(15) Kambe, S.; Murakoshi, K.; Kitamura, T.; Wada, Y.; Yanagida, S.; Kominami, H.; Kera, Y. *Sol. Energy Mater. Sol. Cells* **2000**, *61*, 427−441.

(16) Wood, P. M. *FEBS Lett*. **1974**, *44*, 22−24.

(17) Tang, H.; Berger, P. E.; Schmid and Levy. F. *Solid State Commun*. **1993**, *87*, 847−850.